



This is a repository copy of *FGF-2 promotes osteocyte differentiation through increased E11/podoplanin expression*.

White Rose Research Online URL for this paper:  
<http://eprints.whiterose.ac.uk/128992/>

Version: Published Version

---

**Article:**

Ikpeghu, E., Basta, L., Clements, D.N. et al. (6 more authors) (2018) FGF-2 promotes osteocyte differentiation through increased E11/podoplanin expression. *Journal of Cellular Physiology*, 233 (7). pp. 5334-5347. ISSN 0021-9541

<https://doi.org/10.1002/jcp.26345>

---

**Reuse**

This article is distributed under the terms of the Creative Commons Attribution (CC BY) licence. This licence allows you to distribute, remix, tweak, and build upon the work, even commercially, as long as you credit the authors for the original work. More information and the full terms of the licence here:  
<https://creativecommons.org/licenses/>

**Takedown**

If you consider content in White Rose Research Online to be in breach of UK law, please notify us by emailing [eprints@whiterose.ac.uk](mailto:eprints@whiterose.ac.uk) including the URL of the record and the reason for the withdrawal request.



[eprints@whiterose.ac.uk](mailto:eprints@whiterose.ac.uk)  
<https://eprints.whiterose.ac.uk/>

# FGF-2 promotes osteocyte differentiation through increased E11/podoplanin expression

Ekele Ikpegbu<sup>1,2</sup> | Lena Basta<sup>1</sup> | Dylan N. Clements<sup>1</sup> | Robert Fleming<sup>1</sup> |  
Tonia L. Vincent<sup>3</sup> | David J. Buttle<sup>4</sup> | Andrew A. Pitsillides<sup>5</sup> |  
Katherine A. Staines<sup>6</sup>  | Colin Farquharson<sup>1</sup>

<sup>1</sup>Roslin Institute and R(D)SVS, The University of Edinburgh, Edinburgh, UK

<sup>2</sup>Michael Okpara University of Agriculture, Abia, Nigeria

<sup>3</sup>Arthritis Research UK Centre for Osteoarthritis Pathogenesis, Kennedy Institute of Rheumatology, University of Oxford, Oxford, UK

<sup>4</sup>Department of Infection, Immunity & Cardiovascular Disease, The University of Sheffield Medical School, Sheffield, UK

<sup>5</sup>Comparative Biomedical Sciences, The Royal Veterinary College, London, UK

<sup>6</sup>School of Applied Sciences, Edinburgh Napier University, Edinburgh, UK

## Correspondence

Katherine Staines, School of Applied Sciences, Edinburgh Napier University, Edinburgh, UK.  
Email: k.staines@napier.ac.uk

## Funding information

Arthritis Research UK, Grant number: 20413; Biotechnology and Biological Sciences Research Council, Grant numbers: BB/J004316/1, BBS/E/D/20221657; Tertiary Education Trust Fund Nigeria (TETFund)

E11/podoplanin is critical in the early stages of osteoblast-to-osteocyte transitions (osteocytogenesis), however, the upstream events which regulate E11 expression are unknown. The aim of this study was to examine the effects of FGF-2 on E11-mediated osteocytogenesis and to reveal the nature of the underlying signaling pathways regulating this process. Exposure of MC3T3 osteoblast-like cells and murine primary osteoblasts to FGF-2 (10 ng/ml) increased E11 mRNA and protein expression ( $p < 0.05$ ) after 4, 6, and 24 hr. FGF-2 induced changes in E11 expression were also accompanied by significant ( $p < 0.01$ ) increases in *Phex* and *Dmp1* (osteocyte markers) expression and decreases in *Col1a1*, *Postn*, *Bglap*, and *Alpl* (osteoblast markers) expression. Immunofluorescent microscopy revealed that FGF-2 stimulated E11 expression, facilitated the translocation of E11 toward the cell membrane, and subsequently promoted the formation of osteocyte-like dendrites in MC3T3 and primary osteoblasts. siRNA knock down of E11 expression achieved >70% reduction of basal E11 mRNA expression ( $p < 0.05$ ) and effectively abrogated FGF-2-related changes in E11 expression and dendrite formation. FGF-2 strongly activated the ERK signaling pathway in osteoblast-like cells but inhibition of this pathway did not block the ability of FGF-2 to enhance E11 expression or to promote acquisition of the osteocyte phenotype. The results of this study highlight a novel mechanism by which FGF-2 can regulate osteoblast differentiation and osteocyte formation. Specifically, the data suggests that FGF-2 promotes osteocytogenesis through increased E11 expression and further studies will identify if this regulatory pathway is essential for bone development and maintenance in health and disease.

## KEYWORDS

E11/podoplanin, FGF-2, osteoblasts, osteocytes, osteocytogenesis

Katherine A. Staines and Colin Farquharson are the joint senior authors.

This is an open access article under the terms of the Creative Commons Attribution License, which permits use, distribution and reproduction in any medium, provided the original work is properly cited.

© 2017 The Authors. *Journal of Cellular Physiology* Published by Wiley Periodicals, Inc.

## 1 | INTRODUCTION

Osteocytes are derived from osteoblasts and are the most abundant cells, residing in mineralized bone of the adult skeleton. It has long been accepted that osteocytes are formed by the passive entrapment of redundant osteoblasts by osteoid synthesized by their close neighbors (Palumbo, Ferretti, & Marotti, 2004; Skerry, Bitensky, Chayen, & Lanyon, 1989). The transition from the cuboidal-like osteoblastic morphology to a dendritic shape characteristic of an osteocyte is, however, a more active and tightly regulated process than originally recognized (for reviews see Dallas & Bonewald, 2010; Franz-Odenaal, Hall, & Witten, 2006).

The mechanisms which govern this osteoblast to osteocyte transition (osteocytogenesis) are generally unknown but fundamental studies by Bonewald and coworkers identified E11/podoplanin, a mucin-type transmembrane glycoprotein, as the earliest osteocyte marker protein expressed during osteocytogenesis (Zhang et al., 2006). Furthermore, E11 triggers actin cytoskeletal dynamics (Staines et al., 2016), which are required for dendrite formation and transient E11 knockdown blocks dendrite elongation (Zhang et al., 2006). E11 glycoprotein is not unique to bone and is ubiquitously expressed by many tissues in which it has a range of regulatory functions including cell development, differentiation and invasiveness, epithelial-mesenchymal transition, and oncogenesis (Astarita, Acton, & Turley, 2012; Martín-Villar, Yurrita, Fernández-Muñoz, Quintanilla, & Renart, 2009; Thiery, 2002; Wicki & Christofori, 2007). Owing to its wide tissue expression, it is now recognized by several names which include podoplanin in kidney podocytes, T1 $\alpha$  in alveolar type 1 epithelial cells, PA2.26 in skin keratinocytes, gp38 in lymphoid organs, and E11 in lymphatic endothelial cells, osteoblasts, and osteocytes (Breiteneder-Geleff et al., 1997; Farr, Nelson, & Hosier, 1992; Ramirez et al., 2003; Scholl, Gamallo, Vilaró, & Quintanilla, 1999; Wetterwald et al., 1996).

The intracellular signaling mechanisms by which E11 influences dendrite formation involve the activation of the small GTPase, RhoA, and its downstream effector kinase, ROCK (Martín-Villar et al., 2006). ROCK phosphorylates ezrin/moesin/radixin (ERM) and influences the actin cytoskeleton and subsequently cell shape (Martín-Villar et al., 2006, 2014; Sprague, Wetterwald, Heinzman, & Atkinson, 1996). Much less, however, is known about the upstream regulatory events, specifically those that influence levels of E11 expression during osteocytogenesis. Nonetheless, clues from other model systems have indicated that fibroblast growth factor 2 (FGF-2) is able to change chondrocyte gene expression in vitro, including that of E11 (Chong et al., 2013). FGF-2, one of the earliest members identified in the FGF polypeptide family, signals through FGF receptors that have intrinsic tyrosine kinase activity (Powers, Mcleskey, & Wellstein, 2000). In addition to chondrocytes, FGF-2 is expressed by osteoblasts and is stored in the extracellular matrix where it regulates bone formation via influence on progenitor cell lineage commitment and/or osteoblast differentiation (Hurley, Marie, & Florkiewicz, 2002; Montero et al., 2000; Sabbieti et al., 1999; Xiao et al., 2010). Indeed, mice deficient in *Fgf2* have

decreased bone mass and altered trabecular architecture whereas *Fgf2* transgenic mice present with increased bone mineral density and cortical and trabecular thickness, as well as a variety of skeletal malformations including shortening and flattening of long bones (Coffin et al., 1995; Montero et al., 2000; Xiao et al., 2009).

Cognizant of FGF-2 stimulation of E11 expression in cartilage explants and osteoblast-like cells, we, therefore, hypothesized that FGF-2 may influence bone remodeling via increased osteoblast E11 expression and concomitant osteocyte dendrite formation (Chong et al., 2013; Gupta, Yoo, Hebert, Niger, & Stains, 2010). Hence, the aims of this current study were to examine the effects of FGF-2 on E11 expression in osteoblasts during osteocytogenesis and to explore putative signaling pathways controlling this process.

## 2 | MATERIALS AND METHODS

### 2.1 | Animals

FGF-2-deficient mice (KO) were originally created by Tom Doetschman and obtained from the Jackson Laboratory, and were backcrossed onto a C57BL/6J wild-type (WT) background (Chong et al., 2013). Animal experiments were performed after obtaining ethical and statutory approval in accordance with local policy. Mice were maintained in accordance with UK Home Office guidelines for the care and use of laboratory animals.

### 2.2 | MC3T3 cell culture

Murine MC3T3-E1 (subclone 14), pre-osteoblast-like cells (American Type Culture Collection [ATCC], Manassas, VA) were plated at  $1 \times 10^4$  cells/cm<sup>2</sup> in six-well plates and cultured in  $\alpha$ -MEM medium supplemented with 10% (v/v) FBS (Invitrogen, Paisley UK) and 50  $\mu$ g/ml gentamicin (Invitrogen) at 37°C in a humidified atmosphere with 5% CO<sub>2</sub> and the medium was changed every 2–3 days. Cell viability was assessed using a commercially available Alamar Blue kit (Invitrogen) and cell cytotoxicity using an LDH assay according to the manufacturer's instructions (Promega, Southampton, UK).

### 2.3 | Primary osteoblast isolation

Primary calvarial osteoblasts were obtained from 3-day-old WT mice by serial enzyme digestion of dissected calvarial bones according to published procedure (Orriss, Hajjawi, Huesa, Macrae, & Arnett, 2014; Staines, Zhu, Farquharson, & Macrae, 2014). In brief, calvaria were digested in 1 mg/ml collagenase type II (Thermo Fisher Scientific, Loughborough, UK) in Hanks' balanced salt solution (HBSS) for 10 min and the supernatant discarded; then repeat digestion in 1 mg/ml collagenase type II in HBSS for 30 min; 4 mM EDTA for 10 min and finally 1 mg/ml collagenase type II in HBSS for 30 min. After discarding the first digest, the cells were re-suspended in growth medium consisting of  $\alpha$ -MEM supplemented with 10% (v/v) FBS and gentamicin at 50  $\mu$ g/ml. Osteoblasts were seeded at a density of  $1 \times 10^4$  cells/cm<sup>2</sup>, and incubated at 37°C/5%CO<sub>2</sub> with media changes every 2–3 days.

## 2.4 | FGF-2 treatments

When MC3T3 cells and primary osteoblasts were confluent (day 0), the culture media were replaced with  $\alpha$ -MEM supplemented with 1% (v/v) FBS, 50  $\mu$ g/ml gentamicin and 0–50 ng/ml FGF-2 (PeproTech, London, UK) in 0.1% bovine serum albumin (BSA). Each test condition was completed in triplicate.

## 2.5 | Signaling inhibitors

MC3T3 cells were incubated with appropriate concentrations (specific details in results) of the MEK1/2 inhibitor, U0126, the PI3K inhibitor, LY294002 (InvivoGen, Toulouse, France), and the p38 inhibitor, SB203580 (Cell Guidance Systems, Cambridge, UK). These inhibitors have been reported to be selective for these molecules (Choi et al., 2008; Hotokezaka et al., 2002; Macrae, Ahmed, Mushtaq, & Farquharson, 2007). Control cultures contained vehicle (0.1% dimethylsulfoxide, DMSO) only.

## 2.6 | RNA extraction and quantitative real-time PCR (RT-qPCR)

Total RNA was extracted from MC3T3 cells and primary osteoblasts using a Qiagen RNeasy Mini kit (Qiagen, Manchester, UK) according to the manufacturer's recommendations. The RNA samples were reverse-transcribed into cDNA using Superscript II reverse transcriptase (Invitrogen) according to the manufacturer's instructions. RT-qPCR was carried out in a Stratagene Mx3000P cycler with each reaction containing 50 ng template cDNA, 250 nM forward and reverse primers (Supplementary Table S1), and PrecisionPlus Mastermix (Primer Design, Chandler's Ford, UK). The cycle threshold (Ct) values for the samples were normalized to that of *Atp5b* or *Gapdh* (Supplementary Table S1) and the relative expression was calculated using the  $2^{-\Delta\Delta Ct}$  method (Livak & Schmittgen, 2001).

## 2.7 | Western blotting

Cells were scraped in RIPA lysis buffer containing protease inhibitors (Roche, Germany), and protein concentrations were determined using the Bio-Rad protein DC assay (Bio-Rad, Hemel Hempstead, UK). Protein (8–15  $\mu$ g) was separated using a 10% Bis-Tris gel and then transferred to a nitrocellulose membrane and probed with appropriate primary antibody (Supplementary Table S2), and appropriate HRP-linked secondary antibody (Supplementary Table S3). Immune complexes were visualized by chemiluminescence using an ECL detection kit and ECL film (GE Healthcare, Amersham, UK). HRP-conjugated anti  $\beta$ -actin antibody (1:70,000, Sigma, Dorset UK) was used as a loading control. Densitometry analysis of protein was performed using Image J (<https://imagej.nih.gov/ij/>) (Baldari, Ubertini, Garufi, D'orazi, & Bossi, 2015).

## 2.8 | E11 immunofluorescence

MC3T3 cells were plated on cover slips at a density of  $6.3 \times 10^3$  cells/cm<sup>2</sup> and following treatment with FGF-2, were fixed with 4%

paraformaldehyde (PFA) for 15 min, washed in PBS and incubated in blocking buffer (1 $\times$  PBS, 5% normal donkey serum and 0.3% Triton X-100) for 1 hr at room temperature (RT). E11 antibody (Supplementary Table S2) was added to each well (1:900 in 1 $\times$  PBS, 0.3% Triton X-100 and 1% BSA) overnight at 4°C. Control cells were incubated with an equivalent concentration of goat IgG (Supplementary Figure S1). Wells were subsequently incubated with AlexaFluor-conjugated donkey anti-goat secondary antibodies (Supplementary Table S3) in the dark for 2 hr at RT. Glass coverslips were then mounted onto slides using ProLong Gold antifade reagent with DAPI (Thermo Fisher Scientific) for nuclei staining (Dobie, Macrae, Huesa, Van't Hof, & Ahmed, 2014). The slides were finally visualized using a Leica DMRB fluorescence microscope and images were taken with a Leica DFC300 digital color camera (Leica, Milton Keynes, UK).

## 2.9 | Transfection of MC3T3 cells with E11 siRNA

E11 siRNA and scrambled siRNA stocks (Qiagen) were diluted to 10 nM. MC3T3 cells were plated at  $8 \times 10^3$  cells/cm<sup>2</sup> and maintained in reduced serum medium. Cells were transfected as per manufacturer's instructions with complexes of E11siRNA with HiPerFect (Qiagen), while control cells were transfected with either complexes of scrambled siRNA, with HiPerFect; or HiPerFect alone. After 24 hr incubation at 37°C/5%CO<sub>2</sub>, FGF-2 (10 ng/ml) was added for a further 24 hr to the cells containing the siRNA/HiPerFect complexes or the HiPerFect alone.

## 2.10 | Immunohistochemistry

The knee joints of 6-week-old male FGF-2 KO and WT mice (Chong et al., 2013), were fixed in 4% PFA for 24 hr before decalcification in 10% ethylenediaminetetraacetic acid (EDTA) pH 7.4 for approximately 3 weeks at 4°C with regular changes. Tissues were dehydrated and embedded in paraffin wax, using standard procedures, after which they were sectioned at 6  $\mu$ m. Sections were dewaxed in xylene, rehydrated, and incubated at 37°C for 30 min in 1 mg/ml trypsin for antigen demasking. Endogenous peroxidases were blocked by treatment with 3% H<sub>2</sub>O<sub>2</sub> in methanol. E11 and sclerostin antibodies (Supplementary Table S2) were used with appropriate IgG controls and secondary antibodies (Supplementary Table S3). The Vectastain ABC universal kit (Vector Laboratories, Peterborough, UK) was used according to the manufacturer's instructions. The sections were dehydrated, counterstained with haematoxylin and mounted in DePeX. Images were captured with Nikon Eclipse Ni microscope (Nikon, UK), fitted with Zeiss Axiocam 105 color camera (Carl Zeiss). The number of positively stained E11 osteocytes within diaphyseal cortical bone were calculated as a percentage of total osteocytes present.

## 2.11 | Phalloidin staining for cell culture

MC3T3 cells were seeded at  $1 \times 10^4$  cells/cm<sup>2</sup> and when sub-confluent they were treated with 10 ng/ml FGF-2 or 0.1% BSA for

control cultures. After 24 hr, the cells were fixed in 4% PFA, rinsed in PBS and permeabilized in 0.1% (w/v) triton X-100 (Sigma) in PBS for 10 mins, and then rinsed in PBS. The cells were incubated in 200  $\mu$ l of Alexa Fluor 488-conjugated phalloidin (Thermo Fisher Scientific) (5  $\mu$ M in PBS with 2% BSA) in the dark at RT for 3 hr. The cells were imaged on a Zeiss Axiovert 25s inverted microscope and digital imaging system (Carl Zeiss Microscopy, LLC, Oberkochen, Germany).

## 2.12 | Phalloidin staining for histological sections

Femurs were decalcified as described above and then cryoprotected in 30% sucrose (w/v) at 4°C for 48 hr. The femora were cut in the mediolateral plane in serial longitudinal 20  $\mu$ m thick-sections using a cryostat and thaw-mounted on gelatin-coated slides for processing. Slides were dried at room temperature for 45 min, washed in PBS twice for 5 min each, and incubated with 0.1% Triton-X 100 (Sigma-Aldrich) for 30 min and then rinsed with PBS. Slides were then incubated with Alexa Fluor 488-conjugated phalloidin (1:20; Thermo Fisher Scientific) for 1 hr. Bone sections were washed in PBS and mounted in VectaShield (Vector Laboratories). Preparations were allowed to dry at room temperature for 12 hr. Sections were imaged on a Zeiss LSM 710 Laser Scanning Confocal Microscope with 488 nm laser excitation and detection settings from 493 to 634 nm. Z-stacks were produced with optimal Nyquist overlap settings using a 63 $\times$ /1.4na oil immersion lens. Voxel sizes were 0.1  $\times$  0.1  $\times$  1.00  $\mu$ m in x,y,z planes, respectively. A comparable region of interest was analyzed for osteocyte parameters in all samples located in the diaphyseal

cortical bone. Image stacks were imported into Bitplane Imaris 8.2.0 software and algorithms were created with Imaris FilamentTracer to render and measure dendritic processes. Surface rendering was used for osteocyte cell body measurements.

## 2.13 | Statistical analysis

Data are expressed as the mean  $\pm$  standard error of the mean (S.E.M) of at least three replicates per experiment. Statistical analysis was performed by Student's t-test, one-way analysis of variance (ANOVA) or a suitable non-parametric test.  $p < 0.05$  was considered to be significant and noted as \* $p$  values of  $< 0.01$  and  $< 0.001$  were noted as \*\* and \*\*\*, respectively.

## 3 | RESULTS

### 3.1 | FGF-2 promotes osteoblast E11 gene and protein expression

Treatment of MC3T3 cells with 10 ng/ml FGF-2 for 4, 6, and 24 hr stimulated E11 mRNA expression in comparison to control cultures, at all time-points examined ( $p < 0.05$ , Figure 1a). We observed a concomitant increase in E11 protein expression in these cells (Figure 1b). Stimulation of E11 mRNA ( $p < 0.05$ , Figure 1c) and E11 protein (Figure 1d) expression by FGF-2 was similarly noted in primary osteoblast cultures. The levels of FGF-2 induced E11mRNA and protein were more prominent in the MC3T3 cells at the early time points (4 and 6 hr), whereas in primary cells these increases peaked at the later time points (24 hr) (Figure 1).

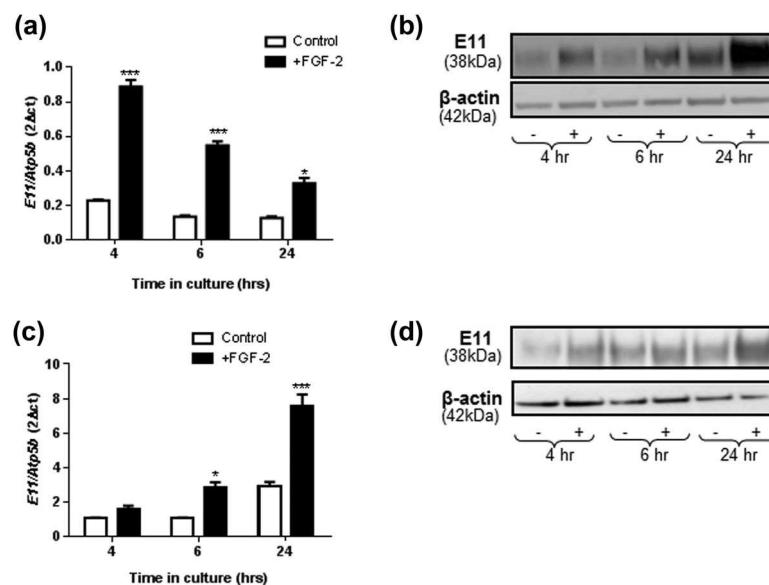


**FIGURE 1** The effect of FGF-2 (10 ng/ml) on (a) E11 mRNA expression and (b) E11 protein expression in MC3T3 cells after 4, 6, and 24 hr challenge, where (+) is FGF-2 treated cell, and (-) is untreated control. The effect of FGF-2 (10 ng/ml) on (c) E11 mRNA expression and (d) E11 protein expression in primary osteoblast cells after 4, 6, and 24 hr challenge, where (+) is FGF-2 treated cell, and (-) is untreated control. Results were normalized to the *Atp5b* housekeeping gene and  $\beta$ -actin for Western loading control. Data are presented as mean  $\pm$  S.E.M for  $n = 3$ ; \* $p < 0.05$ ; \*\*\* $p < 0.001$  compared to untreated cells

### 3.2 | FGF-2 promotes osteoblast-osteocyte differentiation

In light of the increased E11 expression by FGF-2, we next examined the expression of known osteocyte and osteoblast marker genes to determine whether exposure of osteoblast-like cells to FGF-2 promoted osteocytic differentiation. In MC3T3 cells, FGF-2 increased the mRNA expression of the osteocyte marker *Phex* (phosphate regulating endopeptidase homolog, X-linked) at 4 ( $p < 0.01$ ), 6 (not significant), and 24 ( $p < 0.001$ ) hours (Figure 2a). Similarly, *Dmp1* (dentin matrix protein 1) expression was significantly increased at both 6 and 24 hr in MC3T3 cells ( $p < 0.001$ ; Figure 2b). In primary osteoblasts, both *Phex* and *Dmp1* mRNA expressions were also increased by FGF-2 treatment, although the temporal changes were slightly different to those observed in the MC3T3 cells. Specifically, the stimulation of *Phex* expression by FGF-2 was greater at late time points whereas the up-regulation of *Dmp1* was noted at earlier time points when compared with MC3T3 cells (Figures 2c and 2d).

In contrast to the increased expression of osteocyte markers by FGF-2, there was a consistent downward trend in the mRNA expression of the osteoblast markers *Col1a1* (collagen type 1), *Bglap* (osteocalcin), *Alpl* (tissue non-specific alkaline phosphatase), and *Postn* (periostin) in MC3T3 cells treated with exogenous FGF-2 (Figure 3a–d). This down-regulation of osteoblastic marker expression was most consistently observed 24 hr after exposure to FGF-2, although *Alpl* expression was also reduced at 4 ( $p < 0.001$ ) and 6 ( $p < 0.01$ ), as well as 24 ( $p < 0.001$ ) hour time points (Figure 3c). A similar down-regulation of *Col1a1*, *Bglap*, *Alpl*, and *Postn* expression was also observed in FGF-2 treated primary osteoblast cells, which was also most pronounced at longer (24 hr) times following FGF-2

challenge (Figure 3e–h). Together these data indicate that exposure of MC3T3 as well as primary osteoblasts to exogenous FGF-2 promotes early expression of both E11 and osteocyte markers, with a diminution in the expression levels of markers of the osteoblast phenotype following only at later time points.

Assessment of cell viability in the FGF-2 treated MC3T3 cells by the alamar blue assay revealed that after 24 hr of FGF-2 treatment there was no significant differences between the control and FGF-2 treated cells (Figure 3i). We also observed a significant reduction in LDH release in our FGF-2 treated cells ( $p < 0.05$ , Figure 3j) suggesting that there is less cell death. Taken together, these data are consistent with FGF-2 promoting E11 expression and osteoblast-osteocyte differentiation in vitro.

### 3.3 | FGF-2 promotes E11 dependent osteocyte dendrite formation

The differential regulation of osteoblast and osteocyte marker genes, including *E11*, by FGF-2 strongly supports the tenet that FGF-2 can induce osteocytogenesis. To examine this further, we next investigated whether FGF-2 promotes the differentiation of MC3T3 osteoblast-like cells into osteocytes with the adoption of their characteristic dendritic appearance through alterations to the intracellular cytoskeleton. We found that Phalloidin stained control cells displayed a typical rounded morphology with little evidence of dendrite formation (Figure 4a). In contrast, cells treated with FGF-2 for 24 hr displayed numerous delicate dendrites radiating from individual cells and intertwining and connecting with dendrites from neighbouring cells, in a manner characteristic of an osteocyte-like phenotype (Figure 4b). To clarify E11 involvement in this FGF-2

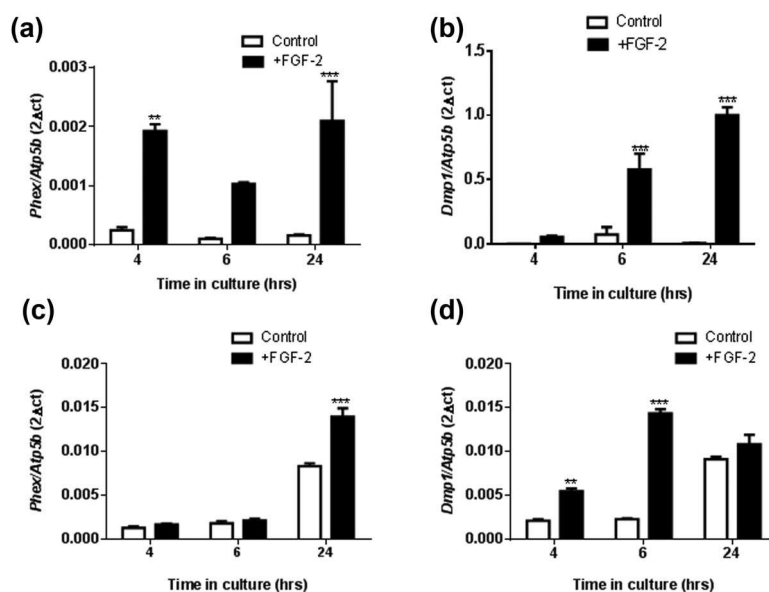


**FIGURE 2** The effect of FGF-2 (10 ng/ml) on the mRNA expression of (a) *Phex* and (b) *Dmp1* in MC3T3 cells after 4, 6, and 24 hr challenge. The effect of FGF-2 (10 ng/ml) on the mRNA expression of (c) *Phex* and (d) *Dmp1* in primary osteoblast cells after 4, 6, and 24 hr challenge. Results were normalized to the *Atp5b* housekeeping gene. Data are presented as mean  $\pm$  S.E.M for  $n = 3$ ; \*\* $p < 0.01$ ; \*\*\* $p < 0.001$  compared to untreated cells

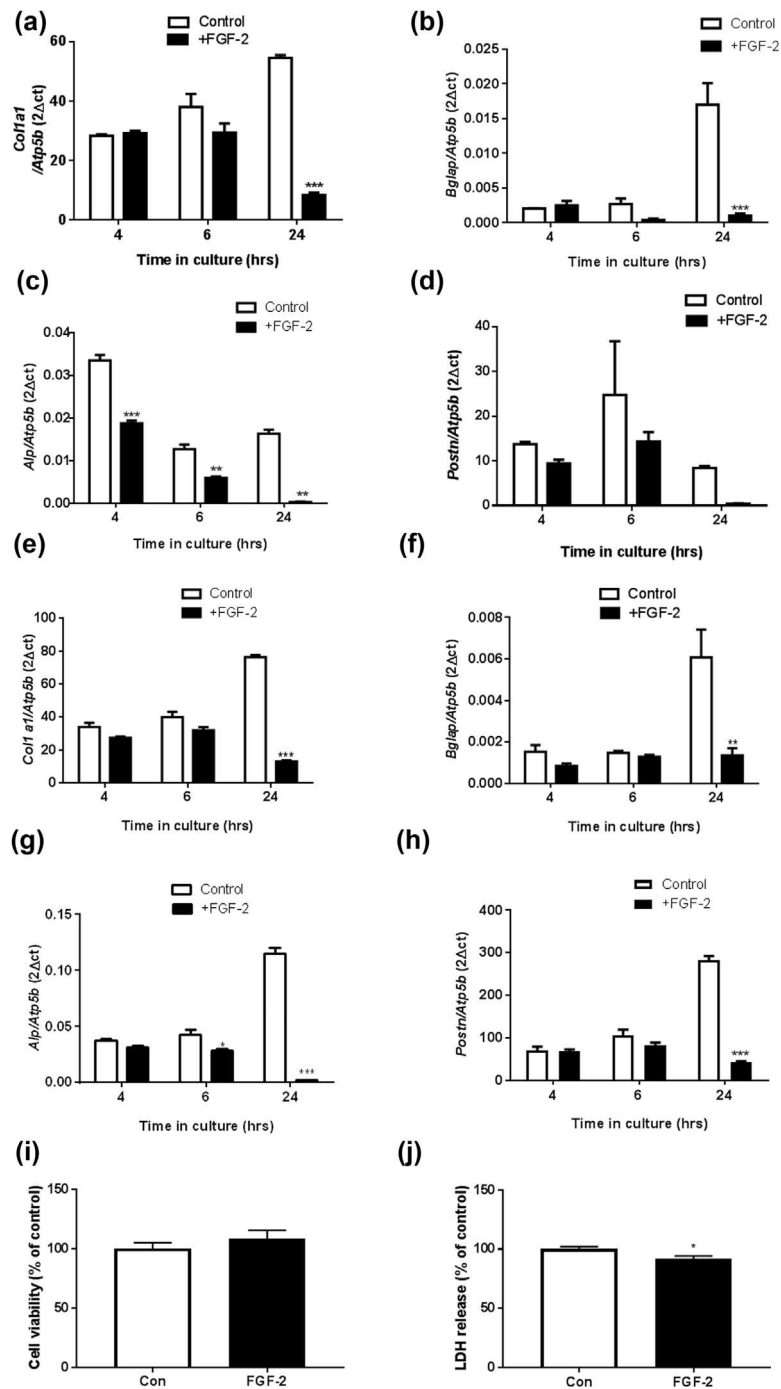


**FIGURE 3** The effect of FGF-2 (10 ng/ml) on the mRNA expression of (a) *Col1a1*, (b) *Bglap*, (c) *Alpl*, and (d) *Postn* in MC3T3 cells after 4, 6, and 24 hr challenge. The effect of FGF-2 (10 ng/ml) on the mRNA expression of (e) *Col1a1*, (f) *Bglap*, (g) *Alpl*, and (h) *Postn* in primary osteoblast cells after 4, 6, and 24 hr challenge. Results were normalized to the *Atp5b* housekeeping gene. (i) Alamar blue assay for cell viability and (j) LDH release assay in FGF-2 treated MC3T3 cells after 24 hr treatment. Data are presented as mean  $\pm$  S.E.M for  $n = 3$ ; \* $p < 0.05$ ; \*\* $p < 0.01$ ; \*\*\* $p < 0.001$  compared to untreated cells

induced change to dendritic phenotype, MC3T3 cells were challenged with FGF-2 for 24–72 hr and immunostained for E11 (Figure 4c). All FGF-2 treated MC3T3 cells exhibited modified morphology with numerous E11 positive dendritic processes radiating from the cell membrane (Figure 4c); these were only rarely observed in control cells. Furthermore, the distribution of

intra-cellular E11 expression changed with both time in culture and FGF-2 treatment. In control cells, it was mostly uniformly distributed within the cytoplasm but after 72 hr in culture, cytoplasmic staining appeared less strong and the predominant staining was associated with focal accumulations at the cell membrane (Figure 4c). This redistribution of E11 to the cell membrane was more obvious and

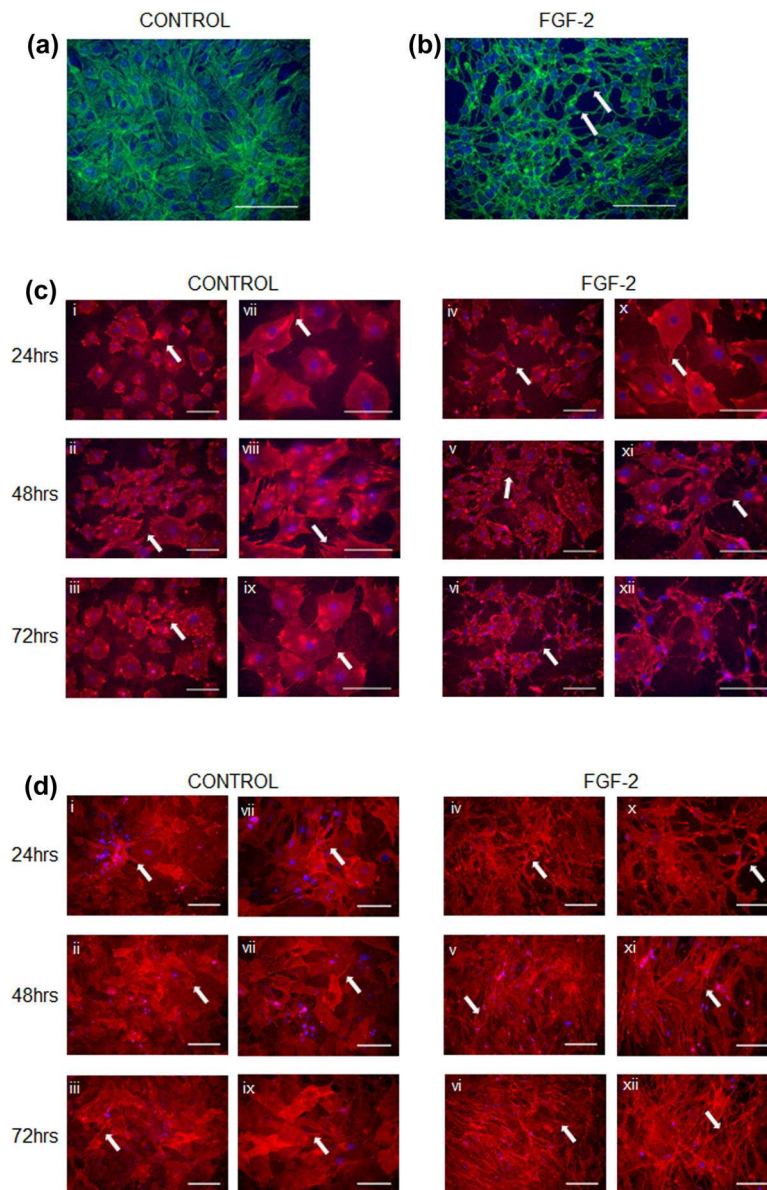


**FIGURE 4** The effect of FGF-2 (10 ng/ml) on MC3T3 osteoblast-like cell morphology. (a) Phalloidin staining for F-actin of control cultures, and (b) FGF-2 treated cultures. Scale bar A & B = 150  $\mu$ m. Immunofluorescence microscopy showing E11 expression and distribution in cells treated with FGF-2 (10 ng/ml) for 24–72 hr in (c) MC3T3, and (d) primary osteoblasts. Note the arrows pointing at the dendrites. Images are representative of three separate experiments. Scale bar c & d (i–vi) = 200  $\mu$ m; c & d (vii–xii) = 150  $\mu$ m

more rapid in the FGF-2 treated cells, where it was achieved within only 24 hr of treatment (Figure 4c). Similarly, FGF-2 promoted dendrite formation and the re-distribution of E11 expression in primary osteoblast cultures (Figure 4d). To determine if the promotion of the osteocyte phenotype by FGF-2 was E11 mediated we studied cells in which MC3T3 cells were transfected with E11 siRNA before being challenged with FGF-2 for 24 hr. E11 gene (77% vs. mock control, 70% vs. scrambled control;  $p < 0.05$ ; Figure 5a) and protein (Figure 5b) expression were silenced successfully by E11 siRNA transfection. Immunofluorescence labeling for E11 and phalloidin staining indicated that compared with mock or scrambled control cell cultures, cells treated with FGF-2 developed less dendrites after silencing of E11 expression (Figures 5c and 5d).

### 3.4 | FGF-2 cell signaling in MC3T3 cells is mediated principally by phosphorylated ERK

FGF receptors (*Fgfr*) 1, 2, and 3, but not *Fgfr4*, were found to be expressed by MC3T3 cells (data not shown). FGF-2 treatment had no effect on *Fgfr1* expression at all-time points studied (Figure 6a), however, it reduced *Fgfr2* ( $p < 0.01$ ; Figure 6b) and *Fgfr3* ( $p < 0.05$ ; Figure 6c) expression after 4 and 24 hr. Treatment of MC3T3 cells with FGF-2 for 15 min revealed that of the pathways examined, there was particularly marked ERK (p44/p42) activation ( $p < 0.001$ ; Figures 6d and 6e), while in comparison there was only slight activation of both Akt ( $p < 0.01$ ; Figures 6d and 6f) and p38 ( $p < 0.05$ ; Figures 6d and 6g), and no effect on JNK phosphorylation (Figures

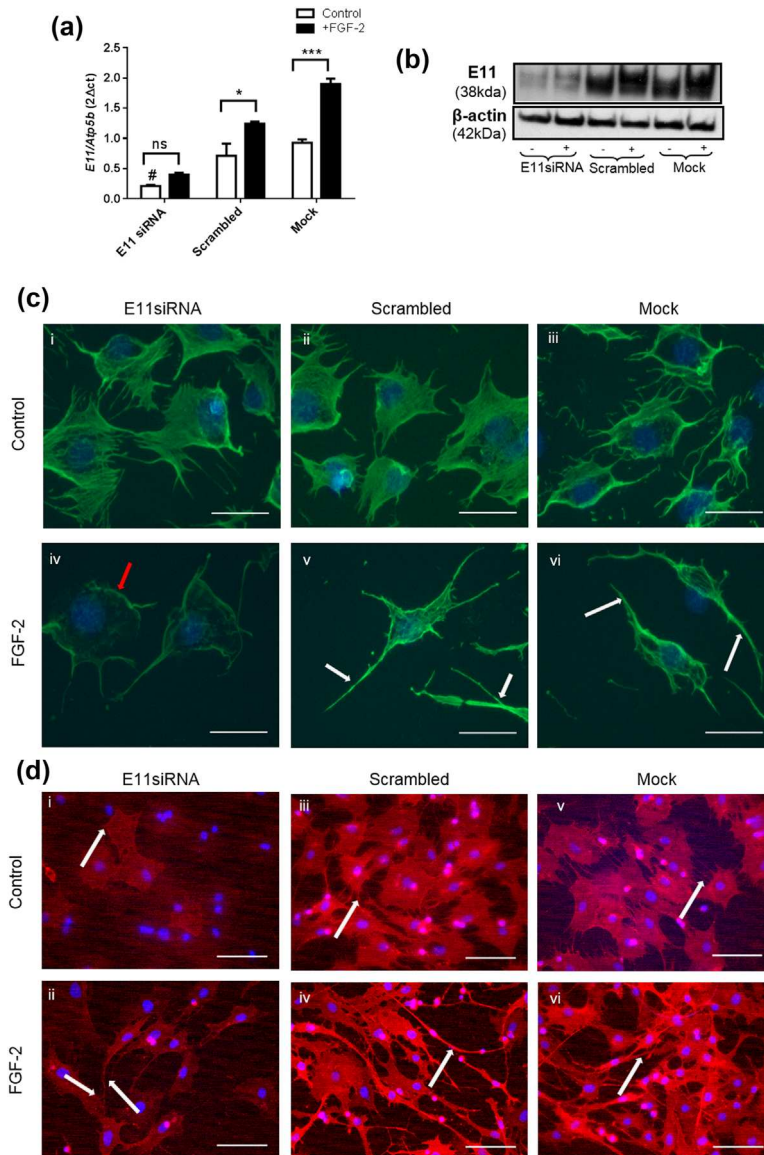


**FIGURE 5** The effect of E11siRNA transfection on FGF-2 (10 ng/ml) stimulation of *E11* (a) mRNA. Results were normalized to the *Atp5b* housekeeping gene. Data are presented as mean  $\pm$  S.E.M for  $n = 3$ ; \* $p < 0.05$ ; \*\*\* $p < 0.001$  compared to untreated control cells; # $p < 0.05$  refers to significant decrease of E11siRNA control when compared to the controls of scrambled and Mock treated cells (b) The effect of FGF-2 (10 ng/ml) on E11 protein expression after E11 siRNA transfection, where (+) is FGF-2 treated cells, and (-) is untreated cells. Results are normalized to  $\beta$ -actin for loading control. (c) Phalloidin staining for F-actin in E11 siRNA, mock and scrambled cultures. Images are representative of three separate experiments. Scale bar = 100  $\mu$ m. (d) Immunofluorescence staining for E11 localization in E11 siRNA, mock and scrambled cultures. Images are representative of three separate experiments. Scale bar = 150  $\mu$ m

6d and 6h). Furthermore, the temporal expression of ERK activation upon FGF-2 treatment revealed a sustained activation over a 48 hr period (Figure 6i), which has been shown previously to be associated with pathways leading to cell differentiation (Pellegrino & Stork, 2006). These data suggest that ERK activation, rather than phosphorylation of alternative Akt, p38, or JNK mediated signaling pathways is likely most influential in regulating E11 downstream of FGF-2.

To further explore the likely role of MEK-ERK signaling in FGF-2 induced differentiation of osteoblast-like cells into osteocytes, we

next treated MC3T3 cells with the ERK inhibitor U0126 (25  $\mu$ M) in the presence or absence of FGF-2 (15 min). While ERK activation by FGF-2 was blunted by U0126 (15 min) treatment (Figure 7a), the prolonged treatment of cells with U0126 (24 hr) did not affect the ability of FGF-2 to enhance E11 gene expression (Figures 7b and 7c). Similarly, treatment of MC3T3 cells with p38 (SB203580) or PI3K (LY294002) inhibitors did not affect the ability of FGF-2 to enhance E11 expression (Figure 7d-g). Further investigations indicated that Akt activation was increased in the presence of MEK inhibition by U0126 and FGF-2 treatment (Figure 7h) and it is possible that this

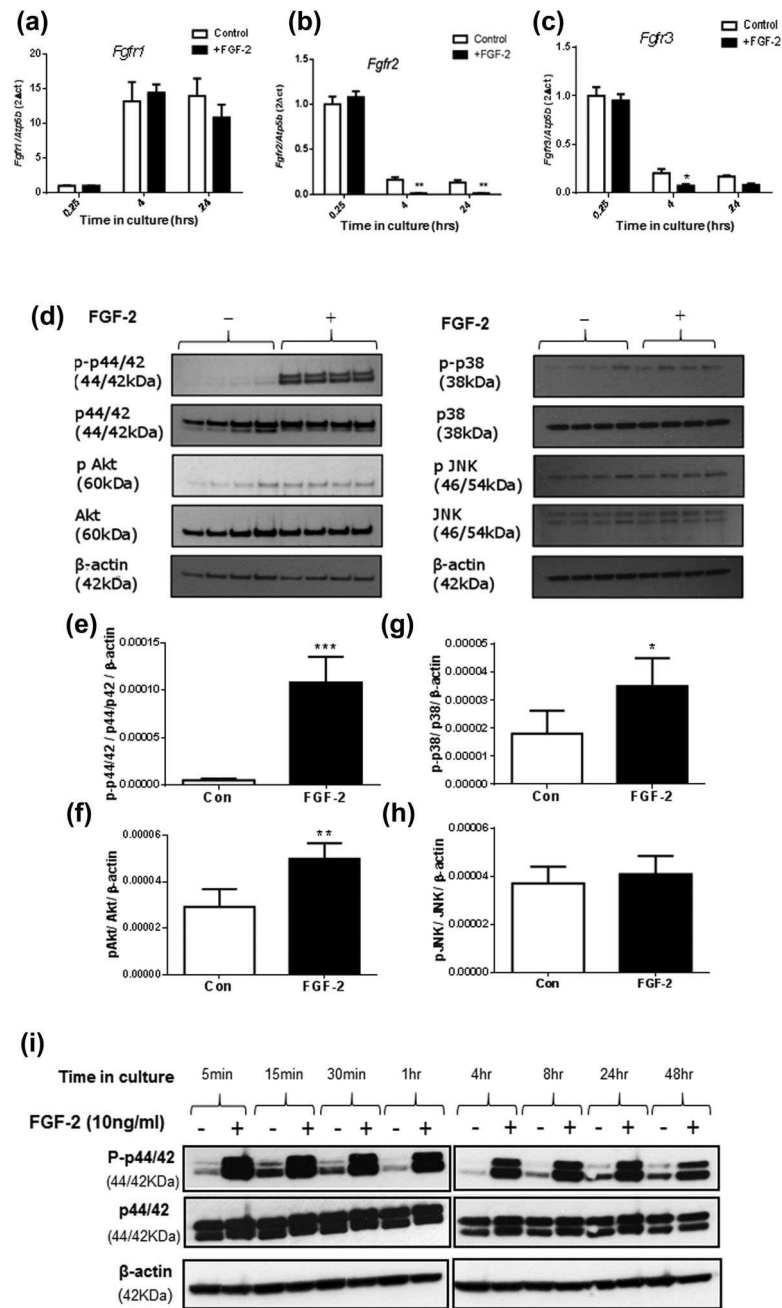


**FIGURE 6** The effect of FGF-2 (10 ng/ml) on the mRNA expression of (a) *Fgfr1*, (b) *Fgfr2*, and (c) *Fgfr3* in MC3T3 cells after 4, 6, and 24 hr challenge. Investigating the downstream signaling pathways involved in FGF-2 stimulation of E11 expression. (d) Western blotting analysis of MC3T3 cells for phosphorylated and total p44/42 (ERK), Akt, p38, and JNK. Densitometry analysis of Western blotting revealed significant upregulation of activated (e) p44/42, (f) Akt, and (g) p38 in treated MC3T3 cells with FGF-2 when compared to control cells. There was no significant increase in (h) JNK expression in both cultures. (i) Western blotting analysis of MC3T3 cells for phosphorylated and total p44/42, in MC3T3 cells treated with FGF-2 when compared to control cells showed an increase in phosphorylated p44/42 in the treated cells at all time points. Results were normalized to the *Atp5b* housekeeping gene and β-actin for Western blotting loading control. Data are presented as mean ± S.E.M for  $n = 4$  and analyzed with student *t*-test. \* $p < 0.05$ ; \*\* $p < 0.01$ ; \*\*\* $p < 0.001$

increased Akt signaling may be a compensatory change to allow FGF-2 to promote E11 expression in the absence of full ERK activation (Figures 7b and 7c). However, the combined inhibition of MEK and PI3K signaling by the inhibitors U0126 and LY294002, respectively, did not affect the ability of FGF-2 to enhance E11 protein expression (Figure 7i).

### 3.5 | Deletion of FGF-2 in vivo results in dysfunctional osteocytogenesis

Finally, we used immunohistochemistry to examine whether FGF-2 KO mice exhibited altered skeletal E11 expression and distribution. Unexpectedly, E11 staining in osteocytes situated within trabecular

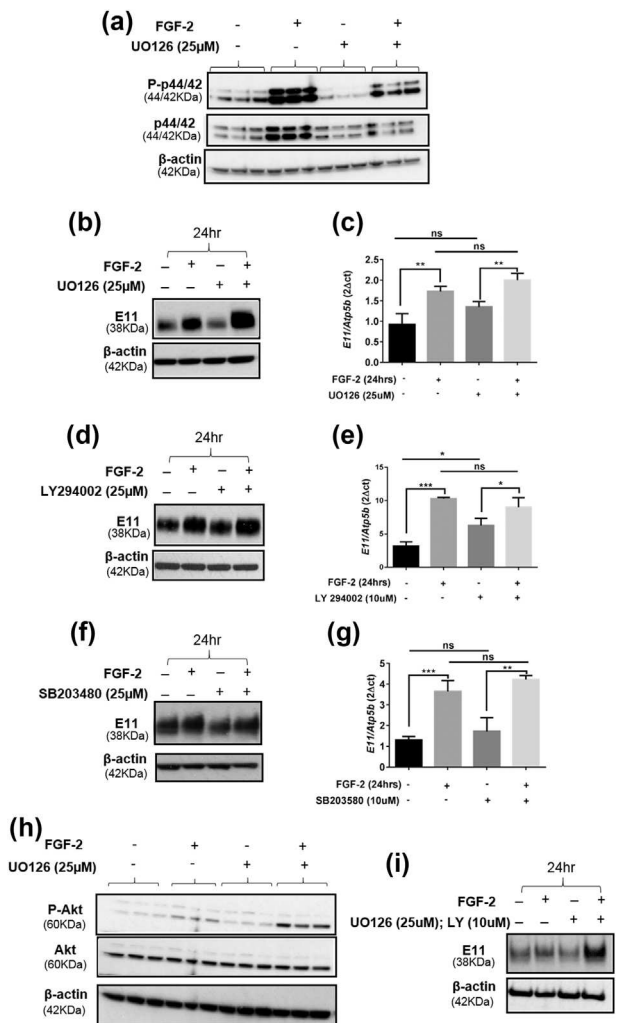


**FIGURE 7** (a) Western blot analysis of ERK signaling in the presence (+) and absence (-) of UO126 (25  $\mu$ m) incubation and subsequent FGF-2 treatment. (b) Western blotting and (c) RT-qPCR analysis of cells stimulated with FGF-2 for 24 hr, in the presence or absence of UO126 (ERK inhibition). (d) Western blotting and (e) RT-qPCR analysis of cells stimulated with FGF-2 for 24 hr, in the presence or absence of LY294002 (Akt inhibition). (f) Western blotting and (g) RT-qPCR analysis of cells stimulated with FGF-2 for 24 hr, in the presence or absence of SB203480 (p38 inhibition). Effect of UO126 (25  $\mu$ m) on Akt protein expression by (h) Western blotting. (i) Effect of UO126 (25  $\mu$ m) and LY294002 (10  $\mu$ m), P-ERK, and P-Akt inhibitors, respectively, on E11 protein expression. Results were normalized to the *Atp5b* housekeeping gene and  $\beta$ -actin for Western blotting loading control. Data are represented as mean  $\pm$  S.E.M for  $n = 3$ . Data are analyzed via one-way ANOVA;  $p < 0.05$  was considered to be significant. \* $p < 0.05$

and cortical bone of FGF-2 KO mice appeared stronger than in osteocytes from WT bones (Figure 8a-d). Quantification of the number of E11 positive cells was, however, similar to those noted in bones from WT mice (Figure 8e). No differences in sclerostin expression or distribution in bones of FGF-2 KO mice in comparison to those from WT mice were observed (data not shown). Histological analysis of osteocyte morphology in FGF-2 KO mice revealed

apparent increases in cell body volume (Figure 8a-d). To confirm and extend these results, we performed phalloidin staining of osteocytes in the cortical bone of FGF-2 KO and WT mice (Figures 9a and 9b). We observed a significant increase in cell body volume ( $p < 0.05$ , Figure 9c) in concordance with our histological observations. Despite this, no differences in cell sphericity were observed (Figure 9d). Similarly, the total number of dendrites (Figure 9e) and the dendrite volume (Figure 9f) were unchanged between FGF-2 KO and WT mice. We did, however, observe a significant decrease in average dendrite volume in FGF-2 KO in comparison to WT mice ( $p < 0.01$ ; Figure 9g), suggestive of dysfunctional osteocytogenesis in FGF-2 KO mice.

## 4 | DISCUSSION

The transmembrane glycoprotein E11, has recently been recognized to be an early driver of the osteoblast to osteocyte transition and the acquisition of the dendritic phenotype (Gupta et al., 2010; Zhang et al., 2006). Consistent with previous data, here we reveal that FGF-2 is able to increase E11 expression and promotes osteocyte dendrite formation, likely independent of intracellular signaling pathways that may involve concomitant FGF-2 induced ERK activation.

Previous brief reports have shown that FGF-2 treatment of osteoblast-like cells induces an increase in E11 expression and the appearance of the osteocyte phenotype (Gupta et al., 2010; Miyagawa et al., 2014). In this present study, we confirm and extend these observations in both MC3T3 osteoblast-like cells and primary osteoblasts. The significant upregulation of *E11*, *Phex*, and *Dmp1* and down-regulation of *Col1a1*, *Bglap*, *Alpl*, and *Postn* in the FGF-2 treated cultures suggests that FGF-2 promotes the differentiation of the osteoblast to the osteocyte stage. Concomitant with this, fluorescence microscopy of cultured cells also disclosed altered E11 expression and localization within the differentiating osteoblast in response to FGF-2. The presence of increased E11 in the cytoplasm and perinuclear area suggests that FGF-2 not only stimulates E11 expression, but also facilitates the translocation of E11 toward the cell membrane. Indeed, the ability of FGF-2 to alter subcellular protein distribution is supported by a previous finding on the expression of *Twist* and *Spry4* proteins in mesenchymal stem cells (Lai, Krishnappa, & Phinney, 2011). Here we observed E11 localization concentrated at the base of the dendritic spikes of the osteocytes after 24–72 hr of FGF-2 treatment. E11 immunofluorescence localization at osteocyte dendritic projections has been reported in MLO-Y4 osteocyte-like cells and primary osteocytes isolated from long bones (Stern et al., 2012). It is, therefore, likely that this redistribution of E11 within the cell is necessary for the transformation of the osteoblast from a cuboidal shape to the osteocytic phenotype characterized by stellate-like morphology with long dendritic processes (Zhang et al., 2006). We also reveal that these morphological changes do not occur because of altered cell proliferation, nor do they precede cell death, therefore, highlighting the role for FGF-2 in regulating E11 expression and osteocyte differentiation in vitro.

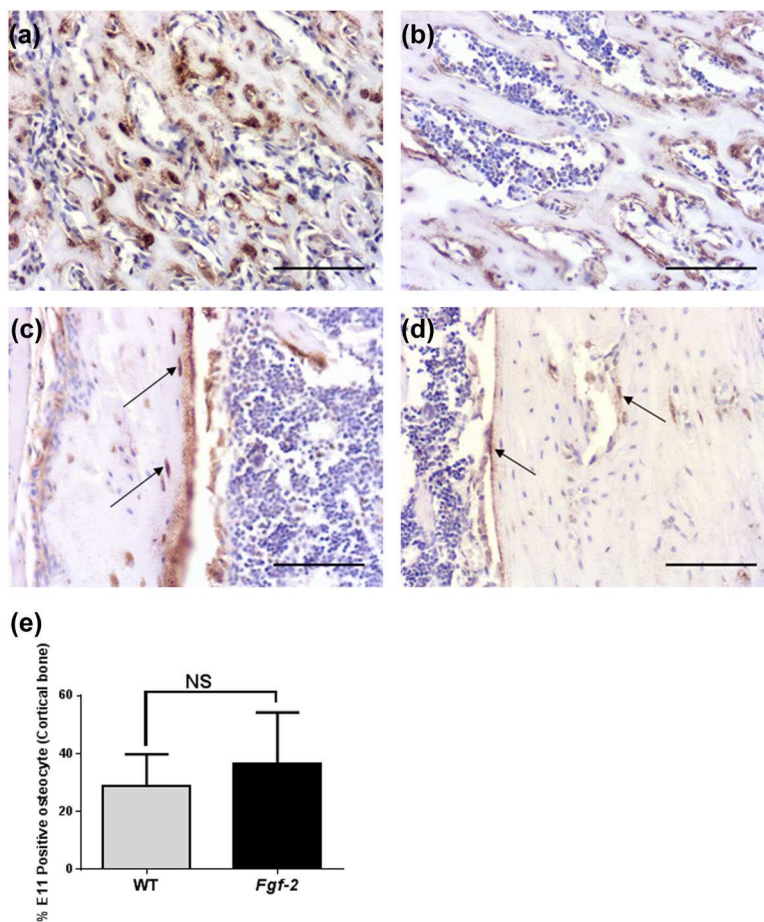


**FIGURE 8** Sections of (a and b) trabecular bone and (c and d) cortical bone osteocytes from *Fgf-2* KO and WT mice immunostained for E11. (a and b) Scale bar = 150  $\mu$ m. (e) The number of E11 stained osteocytes was similar in cortical bone from *Fgf-2* KO and WT mice. Images are representative of three mice

The intracellular effects of FGF-2 are activated via binding to its cell surface receptors, for example, FGFRs which have intrinsic receptor tyrosine kinase activity. Signaling pathways downstream of FGF-2-receptor binding are known to include ERK, p38, Akt, and PKC (Turner & Grose, 2010). Of those examined in the present study, ERK showed the most robust activation in response to FGF-2 in MC3T3 osteoblast-like cells; although p38 and Akt phosphorylation was also significant. Phosphorylation of ERK has been shown to mediate cell proliferation, differentiation, and matrix mineralization in human osteoblasts (Lai et al., 2001; Marie, Miraoui, & Severe, 2012). The sustained activation of the MEK-ERK pathway and phosphorylation of ERK over long time periods suggests a central role for FGF-2 stimulation of cell differentiation (Murphy, Mackeigan, & Blenis, 2003; Pellegrino & Stork, 2006). This is supported by studies that report the importance of ERK signaling in osteoblast initiation and commitment to the differentiation process (Lai et al., 2001), and in osteocyte dendrite formation (Kyono, Avishai, Ouyang, Landreth, & Murakami, 2012). Indeed, the conditional deletion of ERK ablates the formation of osteocytes with characteristic dendritic processes in vivo (Kyono et al., 2012).

Somewhat surprisingly, however, the MEK inhibitor, UO126 was unable to block FGF-2's ability to promote E11 protein expression

despite a significant reduction in ERK activation. Similar results were observed upon inhibition of PI3K/Akt and p38 signaling. These results suggest that alternative pathways may exist by which FGF-2 is able to enhance E11 expression and osteocyte formation. Such pathways may include the activation of p38 and Akt. Previous reports have indicated that activation of p38 is involved in osteoblast differentiation (Hu, Chan, Wang, & Li, 2003) whereas Akt phosphorylation is associated with cell survival (Debiais et al., 2004). The down regulation of Akt by FGF-2 has, however, also been reported in human and mouse cells (Chaudhary & Hruska, 2001). In our hands, however, the dual inhibition of Akt and ERK activation by LY294002 and UO126, respectively, did not result in a block in E11 expression by FGF-2 and further work is required to unravel the signaling pathways that mediate FGF-2 effect on the up-regulation of E11 expression. The lack of JNK activation by FGF-2 in this study is consistent with JNK phosphorylation (P-JNK) mediating late osteoblast maturation (Matsuguchi et al., 2009).

Having shown that FGF-2 promotes E11 expression in MC3T3 osteoblast like-cells and murine primary osteoblasts, it was surprising to note that E11 protein expression by early osteocytes appeared to be increased in sections of bone from *Fgf-2*-deficient mice albeit no

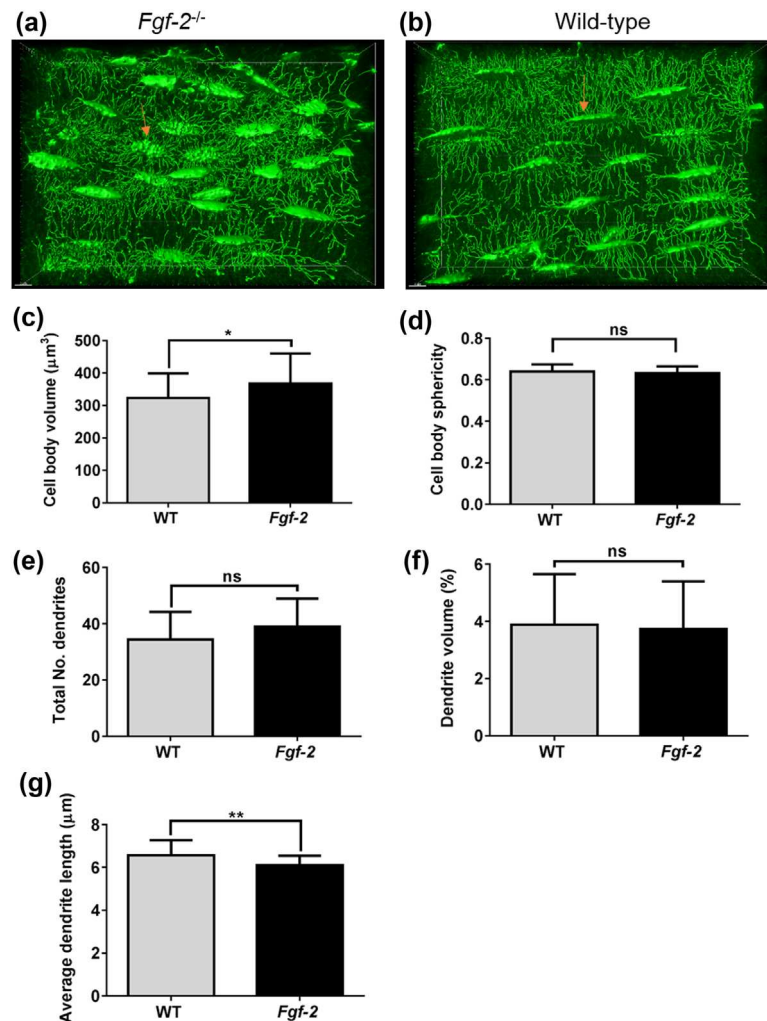


**FIGURE 9** Phalloidin stained *Fgf-2* KO and WT mice tibial cortical bone osteocytes and dendritic processes (arrow). Representative image of cortical bone osteocytes in both *Fgf-2* KO (a) with larger cell body volume than the WT (b) as was confirmed by quantification (c), but no difference in cell spherical shape (d). While the total dendrite number (e) and volume (f), were not significantly different, the average length of the WT was longer than the *Fgf-2* KO (g). Data are presented as mean  $\pm$  S.E.M for  $n = 3$  mice; \* $p < 0.05$ , \*\* $p < 0.01$ . Scale bar = 7  $\mu$ m

differences were noted in the number of E11 stained osteocytes. It is recognized that heparin-like glycosaminoglycans can regulate the signaling behavior of FGF-2 and, therefore, it is a possibility that in our cell culture experiments FGF-2 is more available to the cells due to a less mature extracellular matrix being formed (Padera, Venkataraman, Berry, Godavarti, & Sasisekharan, 1999). Alternatively, the increased E11 staining intensity in the osteocytes from *Fgf-2*-deficient mice is maybe a compensatory response in an attempt to overcome the deficit in FGF-2 related promotion of the osteoblast to osteocyte transition, potentially through the upregulation of other members of the FGF family. Similarly, it may simply be a consequence of the significantly increased cell body volume observed in FGF-2 KO osteocytes. Indeed FGF-2 has been reported to decrease chondrocyte hypertrophy in a murine metatarsal organ culture model and as such, may play a similar role in the formation of the osteocyte (Mancilla, De Luca, Uyeda, Czerwiec, & Baron, 1998). Our phalloidin staining also revealed a significant decrease in average dendrite length in FGF-2 KO mice compared to WT mice; a similar phenotype to that observed in our

bone specific E11 conditional knockout mice (Staines et al., 2017). This, therefore, suggests that the absence of FGF-2 in vivo results in dysfunctional osteocytogenesis.

In conclusion, these data taken together show that FGF-2 promotes the osteocyte phenotype and that this is mediated by increased E11 expression which is redistributed within the differentiating osteoblast. If further studies confirm this regulatory role for FGF-2 in osteocyte formation, we will be in a better position to understand the full repertoire of FGF-2 on bone cell function which may provide insights into the etiology of skeletal disorders such as osteoporosis and osteoarthritis.

#### ACKNOWLEDGMENTS

We are grateful to the Tertiary Education Trust Fund Nigeria (TETFund) for funding this research (EI). We are also grateful to Arthritis Research UK (20413, (KAS) and to the Biotechnology and Biological Sciences Research Council (BBSRC) in the form of an

Institute Strategic Programme Grant (BB/J004316/1; BBS/E/D/20221657) (CF).

## ORCID

Katherine A. Staines  <http://orcid.org/0000-0002-8492-9778>

## REFERENCES

- Astarita, J. L., Acton, S. E., & Turley, S. J. (2012). Podoplanin: Emerging functions in development, the immune system, and cancer. *Frontiers in Immunology*, 3, 283.
- Baldari, S., Ubertini, V., Garufi, A., D'orazi, G., & Bossi, G. (2015). Targeting MKK3 as a novel anticancer strategy: Molecular mechanisms and therapeutic implications. *Cell Death & Disease*, 6, e1621.
- Breiteneder-Geleff, S., Matsui, K., Soleiman, A., Meraner, P., Poczewski, H., Kalt, R., ... Kerjaschki, G. (1997). Podoplanin, novel 43-kd membrane protein of glomerular epithelial cells, is down-regulated in puromycin nephrosis. *American Journal of Pathology*, 151, 1141–1151.
- Chaudhary, L. R., & Hruska, K. A. (2001). The cell survival signal Akt is differentially activated by PDGF-BB, EGF, and FGF-2 in osteoblastic cells. *Journal of Cellular Biochemistry*, 81, 304–311.
- Choi, S. C., Kim, S. J., Choi, J. H., Park, C. Y., Shim, W. J., & Lim, D. S. (2008). Fibroblast growth factor-2 and -4 promote the proliferation of bone marrow mesenchymal stem cells by the activation of the PI3K-Akt and ERK1/2 signaling pathways. *Stem Cells and Development*, 17, 725–736.
- Chong, K. W., Chanalaris, A., Burleigh, A., Jin, H., Watt, F. E., Saklatvala, J., & Vincent, T. L. (2013). Fibroblast growth factor 2 drives changes in gene expression following injury to murine cartilage in vitro and in vivo. *Arthritis & Rheumatism*, 65, 2346–2355.
- Coffin, J. D., Florkiewicz, R. Z., Neumann, J., Mort-hopkins, T., Dorn, G. W., Lightfoot, P., ... O'toole, B. A. (1995). Abnormal bone growth and selective translational regulation in basic fibroblast growth factor (FGF-2) transgenic mice. *Molecular Biology of the Cell*, 6, 1861–1873.
- Dallas, S. L., & Bonewald, L. F. (2010). Dynamics of the transition from osteoblast to osteocyte. *Annals of the New York Academy of Sciences*, 1192, 437–443.
- Debiais, F., Lefevre, G., Lemonnier, J., Le Mee, S., Lasmoles, F., Mascarelli, F., & Marie, P. J. (2004). Fibroblast growth factor-2 induces osteoblast survival through a phosphatidylinositol 3-kinase-dependent, -beta-catenin-independent signaling pathway. *Experimental Cell Research*, 297, 235–246.
- Dobie, R., Macrae, V. E., Huesa, C., Van't Hof, R., & Ahmed, S. F. (2014). Direct stimulation of bone mass by increased GH signalling in the osteoblasts of *Socs2*<sup>-/-</sup> mice. *Journal of Endocrinology*, 223, 93–106.
- Farr, A., Nelson, A., & Hosier, S. (1992). Characterization of an antigenic determinant preferentially expressed by type I epithelial cells in the murine thymus. *Journal of Histochemistry and Cytochemistry*, 40, 651–664.
- Franz-Odenaal, T. A., Hall, B. K., & Witten, P. E. (2006). Buried alive: How osteoblasts become osteocytes. *Developmental Dynamics*, 235, 176–190.
- Gupta, R. R., Yoo, D. J., Hebert, C., Niger, C., & Stains, J. P. (2010). Induction of an osteocyte-like phenotype by fibroblast growth factor-2. *Biochemical and Biophysical Research Communications*, 402, 258–264.
- Hotokezaka, H., Sakai, E., Kanaoka, K., Saito, K., Matsuo, K., Kitaura, H., ... Nakayama, K. (2002). U0126 and PD98059, specific inhibitors of MEK, accelerate differentiation of RAW264.7 cells into osteoclast-like cells. *Journal of Biological Chemistry*, 277, 47366–47372.
- Hu, Y., Chan, E., Wang, S. X., & Li, B. (2003). Activation of p38 mitogen-activated protein kinase is required for osteoblast differentiation. *Endocrinology*, 144, 2068–2074.
- Hurley, M. M., Marie, P. J., & Florkiewicz, R. Z. (2002). Fibroblast growth factor and fibroblast growth factor receptor families. In J. P. Bilezikian, L. G. Raisz, & G. A. Rodan (Eds.), *Principles of bone biology* (pp. 825–851). San Diego, CA: Academic Press, Inc.
- Kyono, A., Avishai, N., Ouyang, Z., Landreth, G. E., & Murakami, S. (2012). FGF and ERK signaling coordinately regulate mineralization-related genes and play essential roles in osteocyte differentiation. *Journal of Bone and Mineral Metabolism*, 30, 19–30.
- Lai, C. F., Chaudhary, L., Fausto, A., Halstead, L. R., Ory, D. S., Avioli, L. V., & Cheng, S. L. (2001). Erk is essential for growth, differentiation, integrin expression, and cell function in human osteoblastic cells. *Journal of Biological Chemistry*, 276(17), 14443–14450.
- Lai, W. T., Krishnappa, V., & Phinney, D. G. (2011). Fibroblast growth factor 2 (Fgf2) inhibits differentiation of mesenchymal stem cells by inducing Twist2 and Spry4, blocking extracellular regulated kinase activation, and altering Fgf receptor expression levels. *Stem Cells*, 29, 1102–1111.
- Livak, K. J., & Schmittgen, T. D. (2001). Analysis of relative gene expression data using real-time quantitative PCR and the 2(-Delta Delta C(T)) Method. *Methods*, 25, 402–408.
- Macrae, V. E., Ahmed, S. F., Mushtaq, T., & Farquharson, C. (2007). IGF-I signalling in bone growth: Inhibitory actions of dexamethasone and IL-1beta. *Growth Hormone and IGF Research*, 17, 435–439.
- Mancilla, E. E., De Luca, F., Uyeda, J. A., Czerwiec, F. S., & Baron, J. (1998). Effects of fibroblastic growth factor-2 on longitudinal bone growth. *Endocrinology*, 139, 2900–2904.
- Marie, P. J., Miraoui, H., & Severe, N. (2012). FGF/FGFR signaling in bone formation: Progress and perspectives. *Growth Factors*, 30, 117–123.
- Martin-Villar, E., Borda-D'agua, B., Carrasco-Ramirez, P., Renart, J., Parsons, M., Quintanilla, M., & Jones, G. E. (2014). Podoplanin mediates ECM degradation by squamous carcinoma cells through control of invadopodia stability. *Oncogene*, 34, 4531–4544.
- Martin-Villar, E., Diego, M., Susanna, C., Yurrita, M. M., Vilaró, S., & Quintanilla, M. (2006). Podoplanin binds ERM proteins to activate RhoA and promote epithelial-mesenchymal transition. *Journal of Cell Science*, 119, 4541–4553.
- Martin-Villar, E., Yurrita, M. M., Fernández-Muñoz, B., Quintanilla, M., & Renart, J. (2009). Regulation of podoplanin/PA2. 26 antigen expression in tumour cells. Involvement of calpain-mediated proteolysis. *International Journal of Biochemistry & Cell Biology*, 41, 1421–1429.
- Matsuguchi, T., Chiba, N., Bandow, K., Kakimoto, K., Masuda, A., & Ohnishi, T. (2009). JNK activity is essential for Atf4 expression and late-stage osteoblast differentiation. *Journal of Bone and Mineral Research*, 24, 398–410.
- Miyagawa, K., Yamazaki, M., Kawai, M., Nishino, J., Koshimizu, T., Ohata, Y., ... Michigami, T. (2014). Dysregulated gene expression in the primary osteoblasts and osteocytes isolated from hypophosphatemic Hyp mice. *PLoS ONE*, 9, e93840.
- Montero, A., Okada, Y., Tomita, M., Ito, M., Tsurukami, H., Nakamura, T., ... Hurley, M. M. (2000). Disruption of the fibroblast growth factor-2 gene results in decreased bone mass and bone formation. *Journal of Clinical Investigation*, 105, 1085–1093.
- Murphy, L. O., Mackeigan, J. P., & Blenis, J. (2003). A network of immediate early gene products propagates subtle differences in mitogen-activated protein kinase signal amplitude and duration. *Molecular and Cellular Biology*, 24, 144–153.
- Orriss, I. R., Hajjawi, M. O., Huesa, C., Macrae, V. E., & Arnett, T. R. (2014). Optimisation of the differing conditions required for bone formation in vitro by primary osteoblasts from mice and rats. *International Journal of Molecular Medicine*, 34, 1201–1208.
- Padera, R., Venkataraman, G., Berry, D., Godavarti, R., & Sasisekharan, R. (1999). FGF-2/fibroblast growth factor receptor/heparin-like glycosaminoglycan interactions: A compensation model for FGF-2 signaling. *FASEB Journal*, 13(13), 1677–1687.
- Palumbo, C., Ferretti, M., & Marotti, G. (2004). Osteocyte dendrogenesis in static and dynamic bone formation: An ultrastructural study. *Anatomical Record Part A Discoveries in Molecular Cellular and Evolutionary Biology*, 278, 474–480.

- Pellegrino, M. J., & Stork, P. J. (2006). Sustained activation of extracellular signal-regulated kinase by nerve growth factor regulates c-fos protein stabilization and transactivation in PC12 cells. *Journal of Neurochemistry*, 99, 1480–1493.
- Powers, C. J., Mcleskey, S. W., & Wellstein, A. (2000). Fibroblast growth factors, their receptors and signaling. *Endocrine-Related Cancer*, 7, 165–197.
- Ramirez, M. I., Millien, G., Hinds, A., Cao, Y., Seldin, D. C., & Williams, M. C. (2003). T1 $\alpha$ , a lung type I cell differentiation gene, is required for normal lung cell proliferation and alveolus formation at birth. *Developmental Biology*, 256, 62–73.
- Sabbieti, M. G., Marchetti, L., Abreu, C., Montero, A., Hand, A. R., Raisz, L. G., & Hurley, M. M. (1999). Prostaglandins regulate the expression of fibroblast growth factor-2 in bone. *Endocrinology*, 140, 434–444.
- Scholl, F. G., Gamallo, C., Vilaró, S., & Quintanilla, M. (1999). Identification of PA2.26 antigen as a novel cell-surface mucin-type glycoprotein that induces plasma membrane extensions and increased motility in keratinocytes. *Journal of Cell Science*, 112, 4601–4613.
- Skerry, T. M., Bitensky, L., Chayen, J., & Lanyon, L. E. (1989). Early strain-related changes in enzyme activity in osteocytes following bone loading in vivo. *Journal of Bone and Mineral Research*, 4, 783–788.
- Sprague, L., Wetterwald, A., Heinzman, U., & Atkinson, M. J. (1996). Phenotypic changes following over-expression of sense or antisense E11 cDNA in ROS 17/2.8 cells. *Journal of Bone and Mineral Research*, 11, S132.
- Staines, K. A., Javaheri, B., Hohenstein, P., Fleming, R., Ikpegbu, E., Unger, E., ... Farquharson, C. (2017). Hypomorphic conditional deletion of E11/Podoplanin reveals a role in osteocyte dendrite elongation. *Journal of Cellular Physiology*, 232, 3006–3019.
- Staines, K. A., Prideaux, M., Allen, S., Buttle, D. J., Pitsillides, A. A., & Farquharson, C. (2016). E11/podoplanin protein stabilization through inhibition of the proteasome promotes osteocyte differentiation in murine in vitro models. *Journal of Cellular Physiology*, 231, 1392–1404.
- Staines, K. A., Zhu, D., Farquharson, C., & Macrae, V. E. (2014). Identification of novel regulators of osteoblast matrix mineralization by time series transcriptional profiling. *Journal of Bone and Mineral Metabolism*, 32, 240–251.
- Stern, A. R., Stern, M. M., Van Dyke, M. E., Jahn, K., Prideaux, M., & Bonewald, L. F. (2012). Isolation and culture of primary osteocytes from the long bones of skeletally mature and aged mice. *Biotechniques*, 52, 361–373.
- Thiery, J. P. (2002). Epithelial-mesenchymal transitions in tumour progression. *Nature Reviews Cancer*, 2, 442–454.
- Turner, N., & Grose, R. (2010). Fibroblast growth factor signalling: From development to cancer. *Nature Reviews Cancer*, 10, 116–129.
- Wetterwald, A., Hoffstetter, W., Cecchini, M. G., Lanske, B., Wagner, C., Fleisch, H., & Atkinson, M. (1996). Characterization and cloning of the E11 antigen, a marker expressed by rat osteoblasts and osteocytes. *Bone*, 18, 125–132.
- Wicki, A., & Christofori, C. (2007). The potential role of podoplanin in tumour invasion. *British Journal of Cancer*, 96, 1–5.
- Xiao, L., Liu, P., Li, X., Doetschman, T., Coffin, J. D., Drissi, H., & Hurley, M. M. (2009). Exported 18-kDa isoform of fibroblast growth factor-2 is a critical determinant of bone mass in mice. *Journal of Biological Chemistry*, 284, 3170–3182.
- Xiao, L., Naganawa, T., Lorenzo, J., Carpenter, T. O., Coffin, J. D., & Hurley, M. M. (2010). Nuclear isoforms of fibroblast growth factor 2 are novel inducers of hypophosphatemia via modulation of FGF23 and KLOTHO. *Journal of Biological Chemistry*, 285, 2834–2846.
- Zhang, K., Barragan-Adjemian, C., Ye, L., Kotha, S., Dallas, M., Lu, Y., ... Bonewald, L. F. (2006). E11/gp38 selective expression in osteocytes: Regulation by mechanical strain and role in dendrite elongation. *Molecular and Cellular Biology*, 26, 4539–4552.

## SUPPORTING INFORMATION

Additional Supporting Information may be found online in the supporting information tab for this article.

**How to cite this article:** Ikpegbu E, Basta L, Clements DN, et al. FGF-2 promotes osteocyte differentiation through increased E11/podoplanin expression. *J Cell Physiol*. 2017;1–14. <https://doi.org/10.1002/jcp.26345>